Langmuir

ARTICLE

pubs.acs.org/Langmuir

Electrowetting without Electrolysis on Self-Healing Dielectrics

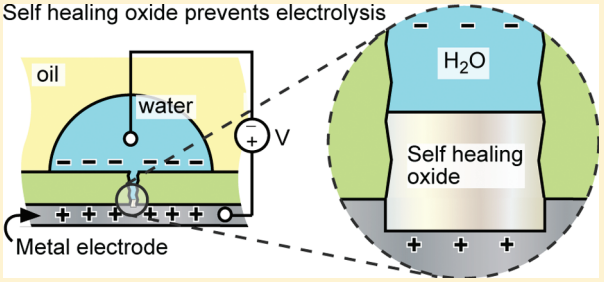
Manjeet Dhindsa,[†,‡] Jason Heikenfeld,[‡] Wim Weekamp,[†] and Stein Kuiper*[,†]

[†]Philips Research Eindhoven, High Tech Campus 34, Eindhoven, The Netherlands 5656 AE

[‡]University of Cincinnati, Novel Devices Laboratory, School of Electronics and Computing, Cincinnati, Ohio 45221, United States

Supporting Information

ABSTRACT: An electrowetting system with protection against dielectric breakdown is presented. It comprises an electrolyte and a Parylene-C film deposited on an aluminum electrode. The system demonstrates virtually instantaneous self-healing (within 100 ms) after dielectric breakdown under both DC and certain AC electrowetting conditions. DC current response during electrowetting on intentionally damaged Parylene-C is presented. Also presented is a characterization of DC offset voltages and duty cycle percentages required for electrolysis free AC electrowetting between 10 Hz and 4 kHz.



INTRODUCTION

Electrowetting on dielectrics[1] continues to receive significant attention as a technique for manipulating liquids for device applications. Despite a large research base, the number of commercially available devices based on electrowetting is still very limited. A primary commercial challenge is preventing short- or long-term breakdown of the thin dielectric layer that separates the conducting liquid from the underlying electrode. The recent trend of going to thinner layers, for voltage reduction, has only exacerbated this issue. Dielectric breakdown can have several causes. Early breakdown may occur at material defects, for instance, pinholes. In order to reduce pinholes, expensive (cleanroom) fabrication must be applied. However, defect-free layers may also break down due to time dependent effects. Electrical fatigue, aging, and long-term interaction with the liquids can lead to destruction of the layer. In order to enhance device durability, the electrowetting system must be capable of withstanding breakdown or instantly recover from such failure. Several material alternatives, such as Parylene HT and liquids free from inorganic ions, have been shown to improve operational stability of electrowetting systems.[2,3] However, these material improvements do not resolve long-term dielectric breakdown or breakdown at major defects.

In this report, we present an electrowetting system that is protected against electrolysis by using a "regenerative" combination of liquid and electrode. An intentionally damaged hydrophobic dielectric layer on aluminum (Al) is demonstrated to instantly recover from electrolysis due to anodization.[4] Such a regenerative system is well-known from electrolytic capacitor technology,[5] where it forms the basis of making and maintaining defect-free dielectric layers. A droplet of conducting liquid is electrowetted under the application of a voltage V, according to the electrowetting equation[6]

$$\cos\theta_V = (\gamma_{os} - \gamma_{as})/\gamma_{ao} + \varepsilon V^2/(2d\gamma_{ao}) \qquad (1)$$

Here, ε is the dielectric constant and d is the thickness of the dielectric, respectively; γ_{ao} is the interfacial tension between the electrowetting liquid (a, typically aqueous), the oil surrounding the electrowetted liquid (o), and the dielectric (s).

Figure 1 shows an electrowetting system with a damaged dielectric. In Figure 1a, the base electrode is the commonly used SnO_2:In_2O_3 (indium−tin-oxide, ITO). It is well-known that for this system the damaged dielectric will result in electrolysis of the aqueous medium. In Figure 1b, the electrode consists of the anodizable aluminum. The damaged dielectric is "repaired" with an insulating oxide layer, thus preventing electrolysis. The key findings of this work are twofold. First, the liquid/electrode materials must be carefully selected to form a highly insulating layer. Second, an electrowetting system is more challenging than a self-anodizing electrolytic capacitor, because electrowetting does not only require defect-free dielectrics, but is also very sensitive to dielectric charging. Such charging can be reduced or prevented by using certain high-quality dielectric coatings or by using AC voltage. AC voltage is problematic for anodization, which only occurs for positive voltage on the electrode. Negative voltage reverses the process (electrochemical etching). We have tackled this additional challenge by modifying the AC voltage for stable and electrolysis free operation. This work provides a general mechanism for improving the reliability of electrowetting systems, and may be of broader use to those exploring anodized dielectrics for electronic devices.

Received: December 31, 2010
Revised: March 3, 2011
Published: April 01, 2011

ACS Publications © 2011 American Chemical Society

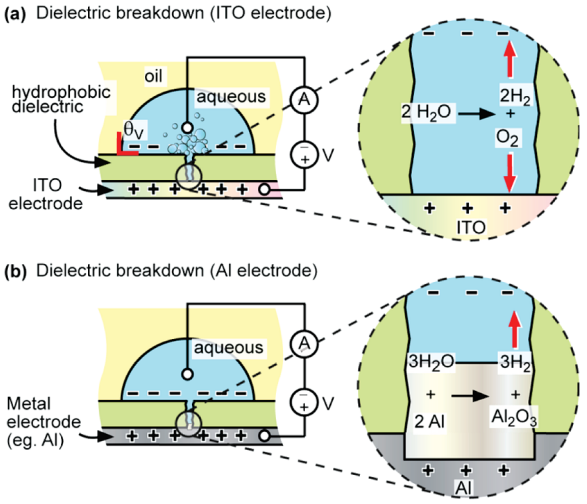


Figure 1. Electrowetting induced dielectric breakdown on an (a) commonly used ITO electrode creates electrolysis; on a (b) anodizable Al anode generates an oxide that blocks and insulates the defect area.

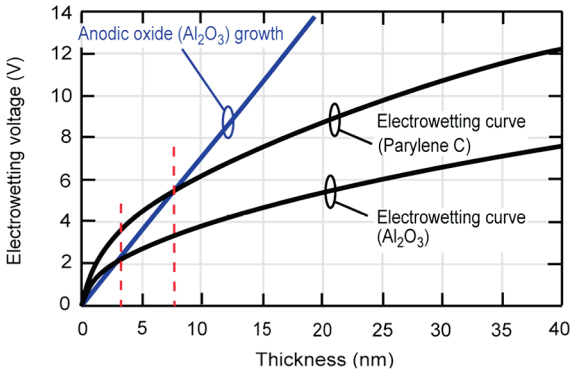


Figure 2. Electrowetting curve (theoretical model of electrowetting voltage vs dielectric thickness) for citric acid in silicone oil on a Parylene-C and Al_2O_3 dielectric, on Al electrode for θ_V =90°. The thickness of anodic oxide for the resulting electrowetting voltages at a growth factor of 1.4 nm V^{-1} is also shown. Electrowetting operation without affecting the dielectric can be performed for Al_2O_3 thicknesses larger than 2.5 nm and Parylene-C thicknesses larger than 7.5 nm.

THEORY

The Anodization Process. The electrowetting system presented herein consists of an anodizable aluminum electrode, a hydrophobic dielectric, an aqueous electrolyte, and an inert platinum (Pt) metal electrode (250 μm in diameter). During dielectric breakdown, a current is generated creating a flux of aqueous H^+ ions toward the cathode and aqueous O^{2-} and OH^- ions toward the anode, while the voltage source supplies a constant voltage. The positive ions combine at the cathode to generate hydrogen gas, whereas the negative ions react with the aluminum to form anodic Al_2O_3. The overall electrochemical reaction is $Al + 3H_2O \rightarrow Al_2O_3 + 3H_2$.[7] The anodization process blocks the current so fast that bubbles are not observed. Hydrogen gas formed during the anodization reaction is created in such small volumes that it is able to dissolve in the liquids. The high electric field drives the mobile O^{2-} and OH^- inside the oxide[7] toward the Al anode to react at the metal/oxide interface and continue Al_2O_3 growth. Similarly, mobile Al^{3+} ions are driven toward the oxide/electrolyte interface and combine with dissociating water molecules to form Al_2O_3. This process of high-field ionic conduction[8] causes anodic Al_2O_3 growth at both interfaces extending into the aluminum by ~30% of its final thickness, as illustrated in Figure 1b. This electrochemical formation of the anodic oxide layer, or constant voltage anodization, is characterized by a sharp increase in current through the metal/electrolyte followed by an exponential decay in current as an insulating oxide layer grows at the interface.

There are several factors that determine properties of the oxide film. First, the current density (J) determines the flux of ions through the oxide, controlling the rate of oxide growth and hence the response of the system to electrolysis (transport rate limited). A larger J results in a quicker oxide formation and therefore a quicker recovery. Second, ionic strength and pH (hydrogen ion activity) of the acidic solution, as well as anodization time and temperature, also determine the overall reaction mechanism and the type of film produced (porous or nonporous).[7] Generally, the concentration of protons (H^+) supplied by the acid regulates the concentration of OH^- ions available to react with the metal and also causes etching/dissolution of the forming Al_2O_3, creating insulated honeycomb-shaped porous structures. Near-neutral solutions with pH 5−7 are commonly used to produce hard nonporous, highly insulating barrier[7] anodic oxide films. Both porous and nonporous films are sufficiently insulating and offer resistance against current flow. Generally, a large current density, as in the case of dielectric breakdown of an electrowetting system, would create a dense nonconducting oxide layer in much less than a second.[9] Also, this anodic oxide continuously self-regenerates during voltage application and will therefore never breakdown.

Electrowetting on Anodically Grown Oxide. Aluminum oxide deposited by atomic layer deposition (ALD) is known to be a good electrowetting dielectric.[2] Aluminum oxide could also be grown directly on aluminum metal via anodization, to serve as a dielectric layer for electrowetting. The total thickness of an anodically grown oxide is linearly dependent on applied voltage.[7] When electrowetting is performed on such anodically grown oxide, it is highly undesirable that the electrowetting voltage causes additional growth of the oxide, as this would alter the performance of the device. Since the electrowetting voltage has a square-root dependence on dielectric thickness (see eq 1), there must exist a critical thickness value above which the electrowetting voltage does not cause additional growth. The question is whether this critical value lies within a range that is practical for application in devices. Figure 2 shows the dependence of electrowetting voltage on dielectric thickness for a 90° contact angle for citric acid (commonly used anodizing electrolyte) in silicone oil on hydrophobized Al_2O_3 dielectric. It should be noted that this theoretical electrowetting curve does not account for the dielectric effects of a fluoropolymer coat, which may dominate for such thin layers.[10] Figure 2 also shows the anodization line, which represents the thickness of anodically grown Al_2O_3 versus voltage at a growth factor of 1.4 nmV^{-1},[7] applied to a common anodization system comprising citric acid and aluminum. From Figure 2, it is evident that in order to obtain stable electrowetting for citric acid (θ_v = 90°) on anodic Al_2O_3 without affecting the electrowetting dielectric, the thickness of this dielectric must be larger than 2.5 nm. Fortunately, even low-voltage electrowetting devices have a dielectric thickness far above this critical value. Typical values used for device applications are 100 nm or more, which shows that in practice the anodic

dx.doi.org/10.1021/la1051468 |*Langmuir* 2011, 27, 5665–5670

Table 1. List of Tests Liquids and Experimentally Measured pH Values

test liquid	pH
deionized (DI H_2O) water	7.1
0.1 M KCl solution	7
8 mM (critical micelle concentration or cmc) sodium dodecyl sulfate (SDS) surfactant solution	5.2
0.38 M citric acid solution	1.6
0.1 M citric acid solution	2.0
0.32 M citric acid/ammonium hydroxide (NH_4OH) solution	6.7
0.38 M citric acid/8 mM SDS solution	2.6

oxide thickness will not be affected during electrowetting operation. It is to be expected that the same conclusion holds for ALD-deposited Al_2O_3, provided that it has been deposited on an aluminum electrode.

Electrowetting on Other Dielectrics. If electrowetting is performed on non-anodized layers deposited on aluminum, such as parylene, the situation is altered. First, the electrowetting curve on parylene is different due to a lower relative dielectric constant (3.1 for Parylene-C versus 8 for Al_2O_3). Second, the Al_2O_3 that grows in a breakdown pore may lift the parylene layer if the aqueous solution is able to penetrate underneath the parylene layer. Figure 2 shows this for the case of Parylene-C.

The intersection point of the electrowetting curve and the anodization line indicates that for Parylene-C the critical value of the thickness is 7.5 nm. This means that, for Parylene-C layers thinner than 7.5 nm, the breakdown-induced Al_2O_3 layer would grow out of the breakdown-induced pore. This value of 7.5 nm is much smaller than the practically used 100 nm, so even if the Al_2O_3 layer fully lifts the parylene layer by growing underneath it, the total dielectric thickness is not affected significantly.

MATERIALS AND EXPERIMENTAL SETUP

Two sets of borosilicate glass substrates were separately sputter-coated with aluminum (Sigma Aldrich, 99.99% pure, 150 nm thick) and transparent conducting ITO (130 nm thick), to form the base electrodes. Aluminum was chosen for this investigation for its low cost and ease of deposition, along with its common use as a reflective electrode for displays.[11,12] Other valve metals such as bismuth (Bi), titanium (Ti), and tantalum (Ta) may also be used as anodizable electrodes instead of aluminum.[13] The electrode-coated substrates were then further coated with a 300 nm Parylene-C dielectric (ε_r = 3.1) using a Specialty Coatings Systems Lab Coater. The Parylene-C samples were then dip-coated with a 30 nm Dupont Teflon AF1600 layer (1% in FC-75, withdraw speed 1 mm s^{-1}). The dielectrics were then purposely damaged for use in several of the anodization experiments. Crosshair (+) shaped patterns were laser-etched through the film stack (including the electrode) using a Nd:YAG frequency doubled laser (λ = 532 nm, 1 kHz). Each etched channel in the crosshair pattern was ~15 μm wide, as limited by laser resolution. A crosshair shape was selected over circular holes, because preliminary tests showed that micrometer-sized holes may become obstructed by gas bubbles that are generated at the base electrode, leading to less reproducible results. The completed substrates were immersed in a silicone oil bath (ABCR-Gelest, polydimethylsiloxane, 5 cSt). A fresh 5 μL droplet of each test solution (electrowetting droplet) was placed into the oil bath and onto each crosshair pattern for testing.

Seven liquids were chosen for testing as listed in Table 1. DI H_2O, KCl, and SDS (sodium dodecyl sulfate) solutions have been extensively used for electrowetting previously.[1,6] The 0.38 M citric acid solution was chosen for its known application in growing and sustaining anodic oxide films in electrolytic capacitors (Internal company data, Philips Research, Eindhoven). The 0.1 M citric acid solution was chosen for its higher pH value for comparison. There are numerous other anodization recipes, typically incorporating weak acids such as tartaric acid, malic acid, and oxalic acid, mixed with NH_4OH (ammonium hydroxide) to neutralize pH (5−7).[7] Therefore, NH_4OH (5.0 N solution) was added to 0.38 M citric acid solution to obtain a 0.32 M citric acid/NH_4OH solution of pH 6.7, and tested. Lastly, the 0.38 M citric acid/8 mM SDS solution was tested to obtain a lower electrowetting voltage (due to a lower γ_{ao}) compared to the citric acid solution without SDS. An oil-phase surfactant (for instance Dow Corning Triton X-15) could also be used here to reduce operating voltage.[14]

The electrical testing equipment included a data acquisition card (NI USB-6259, National Instruments Inc.) programmed to supply a constant voltage (±DC or AC square wave) to the base electrode for 5 s, while the solution droplet was electrically grounded using the Pt probe. The voltage was kept constant to obtain a 90° droplet contact angle, leading to a contact-line radius of approximately 1.3 mm (1.6×10^3 μm^2). AC square wave voltage was varied from 10 Hz to 4 kHz. Current was measured at 10 μs intervals to be able to study the current response within each frequency cycle. The current measurement was capped at ±250 μA due to equipment limitations.

EXPERIMENTAL RESULTS

The positive and negative DC current response for each of the electrowetting solutions under test is shown for an ITO electrode in Figure 3a and an Al electrode in Figure 3b. To obtain $\theta_V = 90°$, the following voltages were applied: ± 32 V DC to the 0.1 M citric acid solution; ± 16 V DC to the 8 mM SDS solution; ± 16 V DC to the 0.38 M citric acid/8 mM SDS solution; ± 30 V DC to all other solutions. All the ITO electrode tests, except low conductivity DI water, showed massive electrolysis and current flow (as expected). For the Al electrodes, solutions that are not known to anodize, or anodizing solutions with the wrong (negative) DC polarity, also showed electrolysis and current flow.

The electrolysis free solutions are now discussed. First, for solutions containing citric acid (but no SDS) a sharp decrease in the current is observed from >250 μA to <14 μA within 0.1 s, to <1.25 μA in 5 s. This is due to the almost instantaneous formation of a 42-nm-thick anodic Al_2O_3 layer, insulating the exposed electrode. Interestingly, as the pH of these solutions increases the rate of current decay also increases and the final current value after 5 s decreases (0.98 μA for 0.1 M citric acid solution and, 0.64 μA for 0.32 M citric acid/NH_4OH solution). This indicates a quicker response, as well as formation of a higher quality barrier oxide for near-neutral solutions. This may be attributed to a decrease in dissolution rate of the forming oxide with increasing pH. For the 8 mM SDS solution, the initial current value is only 90 μA and decreases to 2.73 μA in 5 s. The small initial current value is due to a low ionic concentration and a relatively low applied voltage (16 V). However, there is still growth of a thin oxide and evident decrease in current, possibly due to the slightly acidic nature of the SDS solution (pH 5.2). As

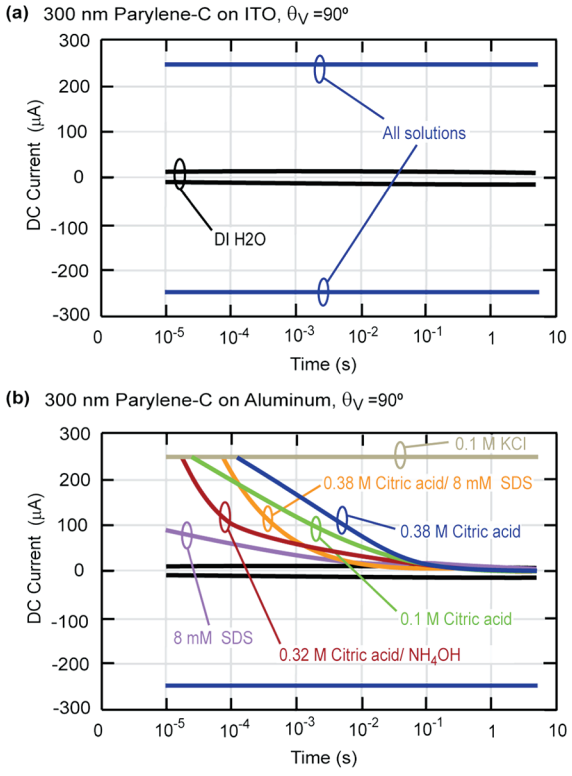


Figure 3. DC current versus time response (5 s) of all test solutions at $\theta_V = 90°$ on laser-etched 300 nm Parylene-C on a (a) ITO electrode and a (b) Al electrode. Positive current values belong to positive voltages and negative current values belong to negative voltages. A decaying current response for the Al electrode in (b) indicates an oxide growth on the Al, with an almost instant response (<0.1 s) for all solutions.

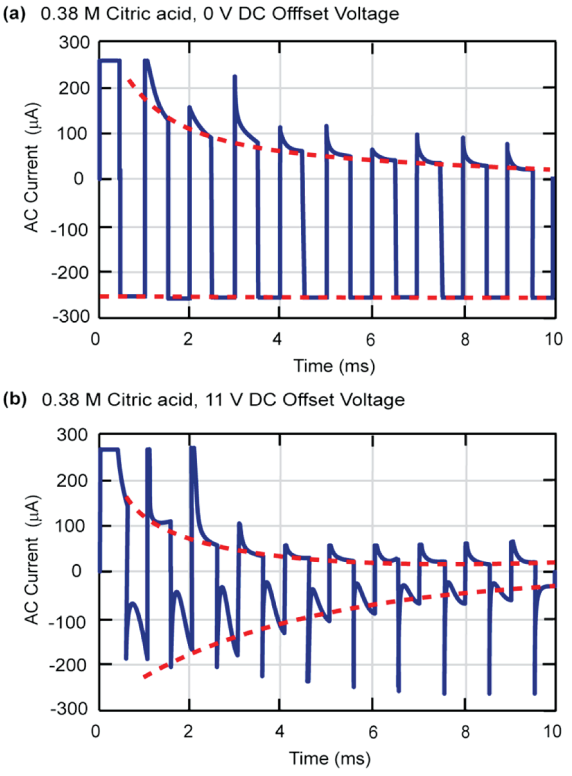


Figure 4. AC current time response (10 ms) of 0.38 M citric acid solution on laser-structured 300 nm Parylene-C on an Al electrode for a 32 V_{rms} 1 kHz AC voltage ($\theta_V = 90°$) and (a) 0 V DC offset voltage, (b) 11 V DC offset voltage. A decaying negative current response in (b) indicates the need for a DC voltage component for complete electrolysis-free AC elctrowetting operation.

would be expected, the response for 0.38 M citric acid/8 mM SDS solution lies perfectly between the responses for 0.38 M citric acid solution and 8 mM SDS solution. It should be noted here that for this solution the final thickness of the anodic Al_2O_3 is 22.4 nm since the operating voltage is now only 16 V (1.4 nm V^{-1}) due to the surface tension lowering properties of the SDS. It was further measured that all of the above solutions except pure water were capable of an electrowetting contact angle modulation larger than 100°.

Next, 0.38 M citric acid solution was tested for AC voltage. As mentioned earlier, citric acid solution is well-established as a stable anodizing solution. In Figure 4, the current response of 0.38 M citric acid solution on laser-structured hydrophobic 300 nm Parylene-C is shown for a 32 V_{rms} 1 kHz AC voltage signal ($\theta_v = 90°$) to the Al electrode. In Figure 4a, an unmodified AC signal is applied. As expected, in the positive cycle, the anodization current, depicted by a dotted trend line, decays exponentially due to an oxide layer buildup. In the negative cycle, this anodic oxide is conducting and quickly dissolves. The negative current remains large (>250 μA in magnitude) as expected. In order to suppress dissolution of the oxide under negative potential, we added a positive DC offset voltage to the AC-signal. In Figure 4b, a DC offset voltage of 11 V is superimposed on the AC signal and the effect of dissolution under a negative bias is overcome within several milliseconds, as can be seen from a decaying negative current trend. Hence, for this offset the system becomes electrolysis-free even under AC voltage and the dielectric recovery is effectively instantaneous. The current peaks that remain visible for both positive and negative polarity are partly due to charging of the capacitor formed by the drop and the underlying electrode.

DC Offset Voltage Optimization. From the above results, it is clear that a DC offset can help to perform electrolysis-free AC voltage electrowetting. Therefore, a characterization of the minimum DC offset voltage required for electrolysis-free AC electrowetting was explored for frequencies ranging from 10 Hz to 4 kHz (Figure 5). The criterion for declaring the response electrolysis-free was chosen to be the fulfillment of two conditions: (1) complete absence of bubble formation; (2) negative current reaching its minimum possible value within 5 s of voltage application. It was observed that increasing the voltage/duty cycle above this threshold value did not decrease the value negative current significantly further, but simply made its decaying response quicker.

Four different AC voltages were tested to ascertain a general trend. Figure 5 depicts the variation in threshold DC offset voltage as a percentage of V_{rms} ($V_{DC}/V_{rms} \times 100\%$) at a constant duty cycle of 50%. Interestingly, for low voltages (7 and 10 V) one can see the required offset voltage decreasing linearly with frequency. In fact, for frequencies above 375 Hz, this value becomes negative. For high voltages (20 and 32 V), the threshold remains constant at ~35%, for all frequencies tested. It should be noted that the reported minimum DC voltage equal to 35% of V_{rms} is all that is required for even an impractically large defect area (1.6×10^3 um^2).

Duty Cycle Optimization. Besides adding a voltage offset, we tried to suppress oxide dissolution by modifying the duty cycle

dx.doi.org/10.1021/la1051468 |*Langmuir* 2011, 27, 5665–5670

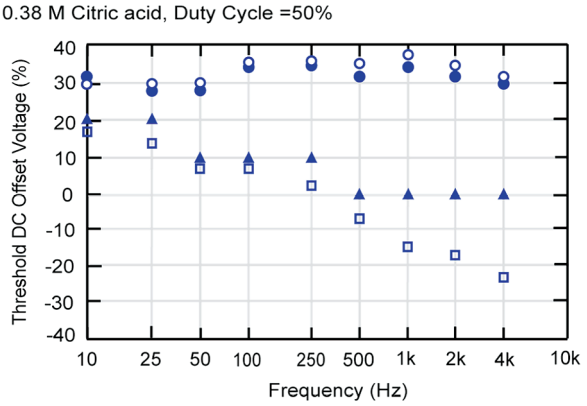


Figure 5. Characterization of threshold DC offset voltage for AC anodic oxide generation for four AC V_{rms} voltages: 32 V (●), 20 V (○), 10 V (▲), 7 V (□).

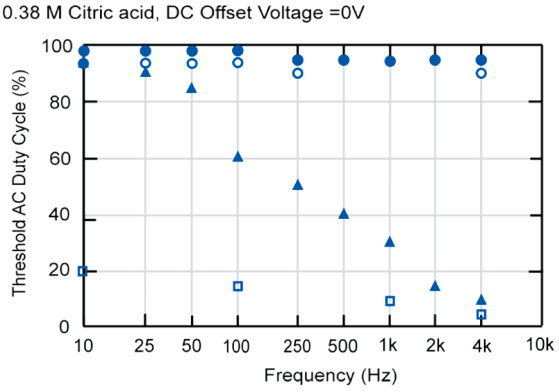


Figure 6. Characterization of threshold AC duty cycle for AC anodic oxide generation for four AC V_{rms} voltages: 32 V (●), 20 V (○), 10 V (▲), 7 V (□).

for the same set of four AC voltages. Figure 6 depicts the threshold duty cycle (%) at 0 V offset. For high voltages, an almost 100% duty cycle is required to prevent electrolysis. For low voltages, a linearly decreasing response, similar to that in Figure 4, is observed. At ~375 Hz, the threshold duty cycle transits to even less than 50%. However, in practical device application, such small voltages (large contact angles) are rarely used. It can therefore be concluded that, in order to perform electrolysis-free AC electrowetting, a DC offset voltage must be used.

Healing from Electrowetting Induced Breakdown. In order to simulate dielectric breakdown in a real world electrowetting device, the citric acid solution droplet was placed on an undamaged hydrophobic 300 nm thick Parylene-C ($E_{Breakdown} \approx 6$ MV cm^{-1}) dielectric film and connected to the ground electrode, while the base electrode (ITO or Al) was subjected to a −90 V DC voltage. A moderate electric field (3 MV cm^{-1}) ensures that there is a controlled initiation of electrically induced formation of conductive pores[2] within the dielectric. Within 6 s, a sharp negative current increase was obtained for both ITO and Al samples, as shown in Figure 7. Current was measured at each 0.5 s interval. A +32 V DC current is then applied to the same drop continuously for 12 s, and an instant decrease in the positive current (approaching 0 μA) is noticed for the Al electrode sample, where as a higher positive current still lingers for the

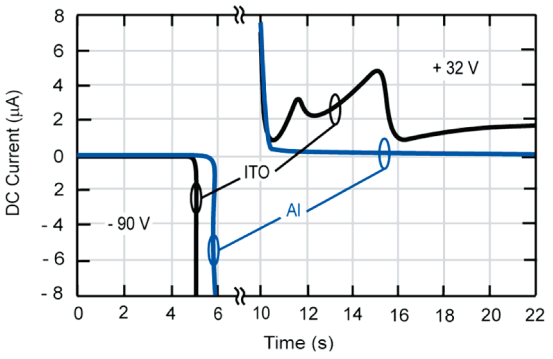


Figure 7. DC current response of the 0.38 M citric acid solution on hydrophobic 300 nm Parylene-C on ITO and Al electrodes. −90 V to the electrodes generates a large current due to electrical damage. +32 V on Al shows healing/recovery from damage via anodic oxide generation.

ITO electrode sample. For the Al electrode, no electrolysis was observed, whereas for ITO, bubble formation was seen to initiate and subsequently worsen over time. It can be concluded that under conditions of natural (electric-field induced) electrowetting breakdown the electrowetting system is capable of instant recovery from electrolysis. It must be noted here that the reversibility of contact angle was preserved without any loss in electrowetted contact angle over the self-healed surface.

Also, a 40-nm-thick Teflon AF1600 film alone coated on Al was shown to sustain stable electrolysis-free electrowetting of a 0.38 M citric acid solution, whereas on ITO, the film breaks down leading to immediate electrolysis. The reader is encouraged to view the videos of this effect provided as a supplement.

Electrowetting on Anodically Grown Al_2O_3. For easy fabrication of electrowetting devices, it would be advantageous to be able to perform electrowetting directly on anodically grown Al_2O_3. We grew several anodic oxide layers and coated them with AF-1600. DC and offset-modified AC electrowetting experiments were performed. Preliminary results of the DC experiments show impractically quick dielectric charging, but the AC (with offset) voltages allowed continuous electrowetting for more than 1.5 h without charging or electrolysis. It should be noted that AC voltage without offset caused electrolysis within the first 15 min on the same system. In anodization, many variables can be tuned and we expect that it is possible to grow layers that also support DC electrowetting.

CONCLUSIONS AND OUTLOOK

This study demonstrates for the first time a new electrolysis-free electrowetting system utilizing the mechanism of anodic oxide generation (anodization) on any exposed portions of the electrode. This system offers complete protection against dielectric breakdown and resulting device failure. It can be simply incorporated into many existing electrowetting devices by the substitution of the electrode by an anodizable electrode and the use of an appropriate acidic or neutral electrolyte solution, under application of a voltage polarity suitable for anodization. A small concentration of a surfactant may be used to reduce the operating voltage. It was demonstrated that the system is capable of sustaining both DC and (modified) AC electrolysis-free electrowetting. For AC driving, it was found that a positive DC voltage offset larger than approximately 35% of the effective AC voltage is required to keep the system electrolysis free.

dx.doi.org/10.1021/la1051468 |*Langmuir* 2011, 27, 5665–5670

It is envisaged that highly insulating anodic oxides, similar to those used in electrolytic capacitors[5] and recently in gate dielectrics for FETs,[15] may also be grown directly on bare (valve metal) electrodes for electrowetting. This is attractive for simpler fabrication and more reliable operation of commercial devices, such as liquid lenses,[16] bio lab-on-a-chip,[17] and, electrowetting and electrofluidic displays.[11,12]

■ ASSOCIATED CONTENT

Supporting Information. Video of damage and self-healing while electrowetting a 0.38 M citric acid drop on top of 300 nm Parylene-C on Al electrode is provided. Video of electrowetting a 0.38 M citric acid drop on 40 nm Teflon on ITO electrode in silicone oil is provided. Video of electrowetting a 0.38 M citric acid drop 40 nm Teflon on Al electrode in silicone oil is provided. This material is available free of charge via the Internet at http://pubs.acs.org.

■ AUTHOR INFORMATION

Corresponding Author
*Stein.Kuiper@Philips.com, Tel. +31 40 2747886.

■ REFERENCES

(1) Berge, B. *C. R. A. S. III* **1993**, *317*, 157–163.
(2) Raj, B.; Dhindsa, M.; Smith, N. R.; Laughlin, B.; Heikenfeld, J. *Langmuir* **2009**, *25* (20), 12387–12392.
(3) Dhindsa, M.; Heikenfeld, J.; Kuiper, S. *Thin Solid Films* **2011**accepted.
(4) Thompson, G. E.; Wood, G. C. In *Treatise on Materials Science and Technology*, Scully, J. C., Ed.; Academic Press: New York, 1983; Vol. 23.
(5) Franklin, R. W. *Proc. lnst. Elec. Eng. Suppl.* **1961**, *109* (22), 525–536.
(6) Mugele, F.; Baret, J.C . *J. Phys.: Condens. Matter* **2005**, *17*, R705–R774F.
(7) Sulka, G. D. In *Nanostructured Materials in Electrochemistry*, Eftekhari, A., Ed.; Wiley-VCH: Weinheim, 2008.
(8) Cabrera, N.; Mott, N. F. *Rep. Prog. Phys.* **1948**, *12*, 163–184.
(9) Ozawa, K.; Majima, T. *J. Appl. Phys.* **1996**, *80* (10), 5828–5836.
(10) Kuiper, S.; Hendriks, B. *Proc. ESA Annual Meeting* **2005**, 28–36.
(11) Hayes, R.; Feenstra, B. J. *Nature* **2003**, *425*, 383–385.
(12) Heikenfeld, J.; et al. *Nat. Photonics* **2009**, *3* (5), 292–296.
(13) Lohrengel, M. M. *Mater. Sci. Eng., R* **1993**, *11* (6), 243–294.
(14) Chevalliot, S.; Dhindsa, M.; Kuiper, S.; Heikenfeld, J. *J. Adhes. Sci. Technol.* **2011**in press.
(15) Dang, X. D.; Plieth, W.; Richter, S.; Plotner, M.; Fischer, W. J. *Phys. Status Solidi A* **2008**, *85*, 1128–1130.
(16) Kuiper, S.; Hendriks, B. H. W. *Appl. Phys. Lett.* **2004**, *85*, 1128–1130.
(17) Dhindsa, M.; Heikenfeld, J.; Kwon, S.; Park, J.; Rack, P. D.; Papautsky, I. *Lab Chip* **2010**, *205* (3), 626–632.